Height Control in Laser Cladding Using Adaptive Sliding Mode Technique: Theory and Experiment

Meysar Zeinali
e-mail: zeinali@uwaterloo.ca

Amir Khajepour
e-mail: akhajepour@uwaterloo.ca

Department of Mechanical and Mechatronics Engineering,
University of Waterloo,
Waterloo, ON, N2L 3G1, Canada

A closed-loop control of the laser cladding process is desired due to difficulties encountered in depositing a layer with acceptable quality from both geometrical and metallurgical point of views. One of the main parameters to achieve the desired geometry in laser cladding process is the height of the deposited layers. In this paper, a real-time measurement and control of the clad height is presented. Due to complex nature of the process and presence of uncertainties, a robust and adaptive sliding mode control is proposed and implemented to control the clad height. The velocity of the substrate is used as a control input while the molten pool height, which is obtained using a charge-coupled device (CCD) camera and an image processing algorithm is used as a feedback signal. Stability of the controller is proven in the presence of time-varying uncertainties and the performance of the closed-loop system is validated by simulation and experiments. The experimental results are promising and show that the geometrical accuracy of the deposited layers can be improved significantly. [DOI: 10.1115/1.4002023]

1 Introduction

Laser cladding by powder injection is a revolutionary method of materials deposition onto a substrate. In this method injected powder is melted by a laser beam in order to coat the surface of a substrate or fabricate near-net shape components. The deposited layer can have a thickness of 0.1–2 mm depending on powder composition, and laser power [1]. These features highlight the potential applications of the laser cladding in the aerospace, oil and gas, bio-engineering, and automotive industries. In particular, laser cladding is used in (i) surface coating, which provides protection against corrosion and wear, (ii) in part and tool repair, which increases the lifespan of expensive parts, (iii) in metallic rapid prototyping, which allows fabricating a part with unique features in single step, and (iv) fabrication of biocompatible implants. However, the survey of literature shows that laser cladding process is highly sensitive to variation in parameters such as powder feed rate, laser power, substrate velocity (scanning speed), as well as external disturbances. The high sensitivity to parameters variation and disturbances may significantly affect the quality of the clad. It has also been reported that excessive surface irregularity during the process could cause undesirable defects in the interface between layers after deposition [2–4]. Therefore, in order to achieve a high quality clad, and reduce the cost of process and time needed to adjust the parameters, and protect the process operator from laser radiation, a robust closed-loop control for laser cladding is inevitable. The quality of the constructed components depends on how precisely the deposition geometrical dimension and mechanical properties can be controlled. In an ideal deposition case, a uniform clad can be obtained, provided that a uniform supply of material and constant energy input are maintained. However, in a real process, irregular powder flow rate due to difficulties involved with powder mass flow control, and laser power fluctuations due to thermal absorbability, reflection and optical instability often result in undesirable deposition [5]. In case of surface coating and repair of components by laser cladding process, maintaining a desired geometry will be an important issue due to irregularities with unknown shape and depth in the surface of the component to be repaired. The laser cladding process and surface irregularities are illustrated in Fig. 1.

The design and implementation of the closed-loop control systems has been reported using different control input, such as powder feed rate [5], laser power [6], melt pool temperature [7], and scanning speed [8,9]. Process modeling based on the input-output data, specifically the dependency of the clad geometry on the process parameters, has also been reported in a very limited research work [1]. Due to the complexity and multidisciplinary nature of laser cladding process arising from the integration of laser machine, positioning system (e.g., multi-axis computer numerically controlled (CNC) machine), powder injection system, feedback device (e.g., CCD camera), and material processing aspect, a robust and reliable model-based control strategies have not yet been fully developed or reported in the literature.

The robust sliding mode controllers (SMCs) have widely been used in practical applications due to their capability to deal with uncertainties, good transient performance and their simplicity [10,11]. But the discontinuous nature of the control law of SMC creates "chattering," which causes damages to the mechanical and electrical components and may excite unmodeled high-frequency dynamics of the system. The widely adopted approach to eliminate the chattering phenomena is the boundary layer method, which require a trade-off between performance and chattering and it is also very difficult to determine the thickness of boundary layer correctly in most cases. Moreover, a priori knowledge of the upper and lower bounds of the uncertainties (i.e., worst-case scenario) is required to obtain robustness and convergence [10–12], and the controller design based on the worst-case scenario may be overly conservative. In order to overcome the drawbacks of the traditional SMC (i.e., chattering, requirement for a priori knowledge of the bounds of uncertainties, and determining the thickness of boundary layer), the SMC design based on estimated uncertainties instead of using the upper and lower bounds of the uncertainties was investigated in Refs. [13–16]. However, an adaptive and chattering-free SMC based on estimated uncertainties are not fully developed and due to a lack of a unified systematic approach is remained mainly unsolved.

Contributed by the Manufacturing Engineering Division of ASME for publication in the JOURNAL OF MANUFACTURING SCIENCE AND ENGINEERING. Manuscript received June 24, 2009; final manuscript received June 7, 2010; published online August 6, 2010. Assoc. Editor: Wei Li.

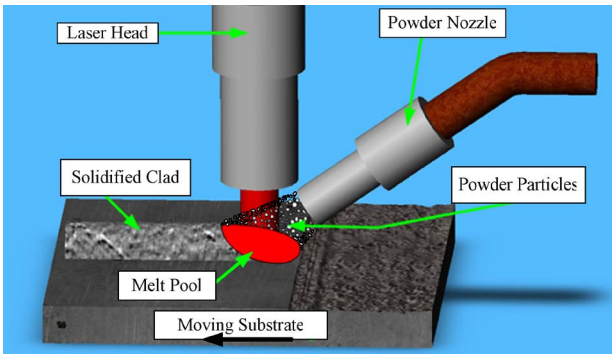

Fig. 1 Schematic of laser cladding process and substrate surface roughness

In this paper, an adaptive and chattering-free SMC based on estimated uncertainties is proposed for laser cladding process. An on-line estimation of uncertainties is proposed using the dynamic behavior of a sliding function. The formulation of the proposed uncertainty estimator consists of two terms: the proportional term and the integral term, which are derived from the systematic stability analysis of the closed-loop system using Lyapunov stability method in Secs. 4 and 5. The uncertainties estimated by a proportional-integral type formulation are used to replace the discontinuous component, also called the switching component, of the standard sliding mode control. This, in turn, eliminates the chattering phenomenon (i.e., high-frequency oscillation) and the requirements for the upper bounds of the uncertainties.

The remainder of this paper is organized as follows. Section 2 presents the experimental setup used to validate the performance of the proposed method. The system description and problem formulation is presented in Sec. 3. Section 4 describes the adaptive sliding mode control (ASMC) design methodology. The stability, and robustness analysis of the proposed controller is presented in Sec. 5. The simulation results are also presented in this section to show the stability and performance of the proposed method in the presence of time-varying uncertainties. The experimental results are presented in Sec. 6. Section 7 concludes this paper.

2 Experimental Setup and System Hardware

The experimental setup for laser cladding process is shown in Fig. 2. The main components of the system are 1 KW fiber laser system integrated with a five-axis CNC machine, a powder feeder system, host and target computers with a four-channel motion control card, and a four-channel image acquisition card from National Instrument. Two extra translational and rotational axes are added to a regular five-axis CNC machine to control the angle of powder delivery nozzle and laser focal point. As shown in Fig. 2, powder is supplied to the melt pool through a lateral nozzle and a CCD camera is used as a feedback sensor to capture the melt pool image and to measure the height of the deposited layer using image processing.

3 System Description and Problem Formulations

Modeling and formulation of laser cladding process has been studied by many researchers. Some of the models are developed to describe the metallurgical aspects of the cladding, such as composition of the alloys and cooling process [17], the calculation of the heat flux in the process [18], and determination of the steady-state temperature [19]. To control the height of the clad, it is of great importance to find relation between melt pool geometry and parameters such as scanning speed, laser power, and powder feed rate. In this regard, Toyserkani et al. [1], developed a Hammerstein–Wiener model, which describes the clad height as function of the scanning speed, Frenk et al. [2] developed a steady-state model, which describes the variation in the clad height based on laser beam velocity (scanning speed) and powder efficiency, Han et al. [3] developed a dynamic model that can be solved using semi-implicit finite-difference method and through an iterative steps, and Fathi et al. [8] proposed a first-order parameterized dynamic model also called gray-box model, which describes the clad height as a function of the scanning speed. However, for real-time control application a computationally efficient and yet accurate dynamic model is required. Development of an accurate and yet computationally efficient dynamic model for a laser cladding process is impossible or very difficult due to complex phenomena such as the interaction between powder particle and laser beam, fluctuating in powder delivery system, and melt pool dynamics. Therefore, in this paper the goal is to design a robust adaptive model-based controller, which relies on online estimation of the uncertainties rather than using the conservatively estimated bounds of the uncertainties. For this purpose the first-order dynamic model proposed by Fathi et al. [8], is adopted to design the controller and discuss the stability of the closed-loop system. The adopted model is as follows:

$$\tau\dot{h} + h = \frac{3}{2}\frac{\dot{m}}{\rho w_0}\left(\frac{d_b}{d_p}\left(1 + \frac{h}{d_b}\tan\alpha\right)\cos\alpha\right)^n \frac{k}{v(t)} \tag{1}$$

where h is the clad height (mm) and $\dot{h}$ is the first derivatives of the clad height (mm/s). $\dot{m}$ is the powder flow rate (g/s), ρ is the powder density (g/m3), w_0 is the steady-state values of the clad width (mm), d_p is the powder jet diameter (mm), d_b is the laser beam diameter (mm), α is the angle between the nozzle and the laser beam, $v(t)$ is the scanning speed (substrate speed), and τ, n,

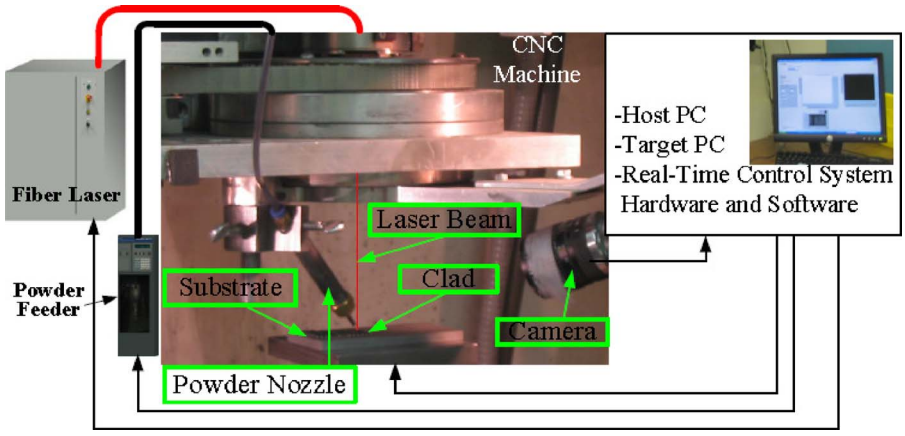

Fig. 2 Configuration of laser cladding setup

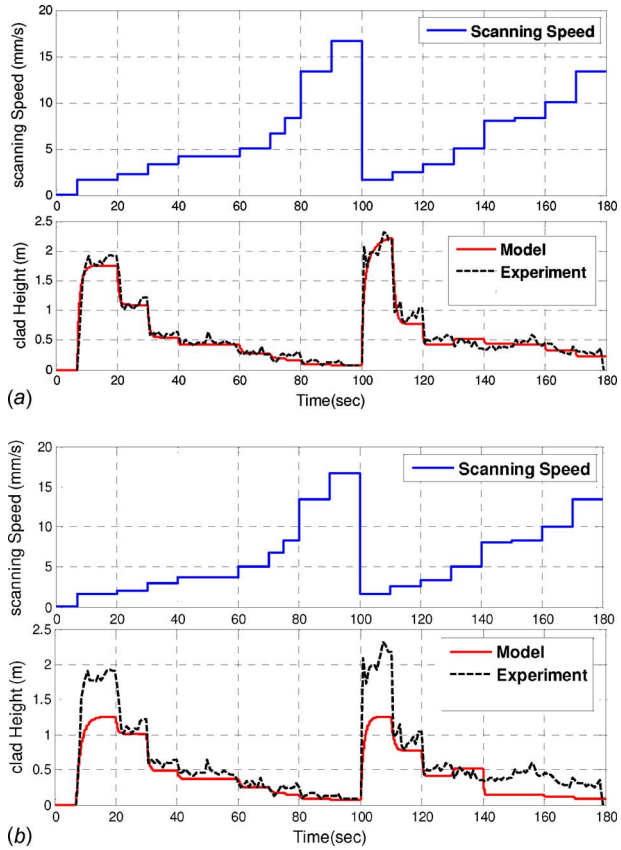

Fig. 3 Comparison of model output and actual process output for: (*a*) well-identified parameters and (*b*) slightly approximated parameters

and k are the unknown parameters that can be identified through the experiment and in an off-line procedure. But to avoid a cumbersome off-line identification procedure, the approximate values of these parameters, which are given in Fathi et al., are used throughout this paper. The error associated with the parameters of the model is considered as a model uncertainty. It will be shown that the robust proposed controller is able to maintain the stability and the desired performance of the closed-loop system in the presence of the parameter uncertainty, external disturbances, and measurement noise. Figure 3(*a*) and 3(*b*) demonstrates the model performance for a two set of parameters τ, n, and k, which are presented in Table 1.

Figure 3(*a*) compares the experimental data and model output for a set of well-identified parameters. Figure 3(*b*) show that a slight change in parameters of the model will cause large error in model output. In order to find the acceptable values of the model parameters, an extensive experimental study and off-line identification are necessary. Laser cladding experiment is very costly and time consuming. On the other hand, laser cladding process is very sensitive to parameters variations and, hence, a set of well-identified parameters for particular materials and powder size may not be suitable for different materials and cladding conditions. In order to avoid a cumbersome and time consuming off-line parameters identification and to deal with unpredicted disturbances, in this paper, the goal is to construct an adaptive control system, which accounts for parameters uncertainties, unmodeled dynamics, and external disturbances.

Table 1 Process and model parameters during simulation and experiments

Parameters description	Set 1	Set 2
Powder flow rate $\dot{m}$ (gr/min)	6	6
Powder density ρ (gr/mm^3)	0.0078	0.0078
Beam diameter d_b on substrate (mm)	1.4	1.4
Powder jet diameter d_p (mm)	2	2
Nozzle angle α (deg)	30	30
Model parameter $\hat{\tau}$	0.5	0.4
Model parameter $\hat{k}$	0.195	0.18
Model parameter $\hat{n}$	2.00	3

The process model presented in Eq. (1) can be expressed as the following familiar form:

$$\dot{x} = f(x,t) + b(x,t)u$$

$$x(t_0) = x_0 \tag{2}$$

where x is the system state and $\dot{x}$ is its first derivative and $x(t_0) = x_0$ is the initial value of x. The scalar $u(t) \in R$ is the control input and $f(x,t) \in R$ is a bounded nonlinear scalar function of the state variable that represents the nonlinear deriving terms. $b(x,t) \in R$ is an invertible and bounded positive definite nonlinear function over entire state space and it can be considered as the control gain. According to Eq. (1), the above mentioned functions are defined as follows:

$$x = h$$

$$f(x,t) = -\frac{h}{\tau} \tag{3}$$

$$b(x,t) = \frac{3}{2}\frac{k}{\tau}\frac{\dot{m}}{\rho w_0}\left(\frac{d_b}{d_p}\left(1 + \frac{h}{d_b}\tan\alpha\right)\cos\alpha\right)^n \tag{4}$$

$$u = \frac{1}{v(t)} \tag{5}$$

Due to unknown parameters τ, n, and k, external disturbances and time-varying parameters (e.g., powder feed rate), the dynamic model of the system is an approximation of the real system. Hence in the presence of uncertainties, functions $f(x,t)$ and $b(x,t)$ are of the form

$$f(x,t) = \hat{f}(h,t) + \Delta f(h,t)$$

$$b(x,t) = \hat{b}(h,t) + \Delta b(h,t) \tag{6}$$

where

$$\hat{f}(x,t) = -\frac{h}{\hat{\tau}}$$

$$\hat{b}(x,t) = \frac{3}{2}\frac{\hat{k}}{\hat{\tau}}\frac{\hat{\dot{m}}}{\rho w_0}\left(\frac{d_b}{d_p}\left(1 + \frac{h}{d_b}\tan\alpha\right)\cos\alpha\right)^n \tag{7}$$

are the known parts, and $\Delta f(.)$ and $\Delta b(.)$ are the unknown parts of $f(.)$ and $b(.)$, respectively. For the sake of simplicity, the arguments of functions f, b, and other functions occasionally are omitted hereafter. Therefore, in the presence of the model uncertainties and external disturbances, Eq. (2) can be written as

$$\dot{h} = \dot{x} = (\hat{f} + \Delta f) + (\hat{b} + \Delta b)u(t) + d(t) \tag{8}$$

where $d(t) \in R$ is the bounded external disturbances. Equation (8) can be rewritten as

$$\dot{h} = \dot{x} = \hat{f} + \hat{b}u(t) + (\Delta f + \Delta b u(t) + d(t)) \tag{9}$$

ASSUMPTION 1. *At this point, it is assumed that the matching conditions are satisfied [20]. This means the uncertainties appear in the same equation as the control input $u(t)$ and the following holds:*

$$\Delta f = \hat{b}\zeta_1; \quad \Delta b = \hat{b}\zeta_2; \quad d(t) = \hat{b}\zeta_3 \tag{10}$$

where ζ_1, ζ_2 , and ζ_3 are unknown function. Then, all uncertain elements can be lumped as [20]:

$$\zeta = \Delta f + \Delta b u(t) + d(t) = \hat{b}(\zeta_1 + \zeta_2 + \zeta_3) \tag{11}$$

By substituting Eq. (11) in Eq. (9), it reduces to

$$\dot{h} = \hat{f} + \hat{b}u(t) + \zeta \tag{12}$$

where ζ represents the lumped uncertainties.

ASSUMPTION 2. *The uncertainty term $\zeta(x,\dot{x},u,t)$ and its partial derivatives are continuous and locally uniformly bounded in Euclidian norm and there exist a nonnegative function $\rho(x,\dot{x},u,t)$, which satisfies the following:*

$$\|\zeta(x,\dot{x},u,t)\| \leq \rho(x,\dot{x},u,t) < \infty \tag{13}$$

Boundedness of ζ is a valid assumption for a large class of physical systems Ref. [21] (page 194) and Ref. [10] (page 304).

4 Adaptive Sliding Mode Controller design

According to Refs. [10,11], the standard sliding mode control law for a nonlinear uncertain system, which guarantees the stability and convergence is a discontinuous and has the following form:

$$u(t) = u_{\text{eq}}(t) - K_b \operatorname{sgn}(S) \tag{14}$$

where $u_{\text{eq}}(t)$ is a model-based component, which is called equivalent control and can be designed based on the approximately known (nominal) dynamics of the system, K_b is the bounds of uncertainty vector, which have to be known a priori, and $\operatorname{sgn}(S)$ is a signum function. However, the application of control law given in Eq. (14) can be limited due to chattering and unknown bounds of the uncertainties.

The discontinuous term $K_b \operatorname{sgn}(S)$ in Eq. (14) is the fundamental cause of chattering and also is designed conservatively based on the bounds of uncertainties K_b. Therefore, in this study, the goal is to replace the discontinuous term with a continuous adaptive term, which can be updated recursively in an online procedure in order to compensate for the uncertainties. This in turn, eliminates the chattering and there is no need to have a priori knowledge of the bound of the uncertainties.

The design of the adaptive continuous sliding mode controller without knowing the bounds of uncertainties consists of two phases: (i) selection/design of a sliding (switching) surface so as to achieve the desired system behavior (e.g., asymptotic stability), when restricted to the surface and (ii) systematically constructing a control law to force the system state trajectory to the sliding surface and maintain it there. This, in turn, guarantees the stability of the closed-loop system [21].

For the first phase of the design, an exponentially stable error dynamics is chosen as a desired sliding surface to guarantee the convergence of tracking error to zero while the system is in the sliding mode. Based on Slotine and Li [10], for a system dynamics defined in Eq. (9), an exponentially stable error dynamics can be defined as follows:

$$S(t) = \left(\frac{d}{dt} + \lambda\right)^{n-1} e = 0 \tag{15}$$

where $S(t)$ is sliding surface function, λ is a positive constant value, and $e=h-h_d$ is the clad height tracking error. The integral type of sliding surface is considered to reduce the tracking error and to ensure zero offset error. For a first-order system integral sliding surface is as follows:

$$S(t) = \left(\frac{d}{dt} + \lambda\right)\left(\int edt\right) = e + \lambda \int edt = 0 \tag{16}$$

The second phase is to design a control law with variable parameters such that it guaranties the existence of sliding mode or makes the associated Lyapunov function a decreasing function of time in the presence of uncertainties. The control law that guarantees achieving the above goals is designed systematically and has the following form:

$$u(t) = u_{\text{eq}}(t) + u_p(t) + u_a(t) \tag{17}$$

where $u_{\text{eq}}(t)$, $u_p(t)$, and $u_a(t)$ are the components of the proposed control law. In what follows it will be shown that $u_p(t)$ and $u_a(t)$ are the continuous components that replace discontinues term $K_b \operatorname{sgn}(S)$ in Eq. (14) and are derived in the sequel. To derive these components the control design phase is divided into three steps as follows.

4.1 Step 1: Equivalent Control Component $u_{\text{eq}}(t)$. In the first step, it is assumed that a sliding mode exists and system dynamics is exactly known. For such a system a continuous model-based law, which is called equivalent control and denoted by $u_{\text{eq}}(t)$ can be designed. The equivalent control term $u_{\text{eq}}(t)$ can be constructed based on the Filippov's equivalent dynamics [10], which states that $\dot{S}(t)=0$ while the dynamics is on the sliding mode. From Eq. (16), the derivative of S is determined as

$$\dot{S} = \dot{e} + \lambda e = \dot{h} - \underbrace{(\dot{h}_d - \lambda e)}_{\dot{h}_r} = 0 \tag{18}$$

where $\dot{h}_r=(\dot{h}_d-\lambda e)$ in Eq. (18) is called reference velocity and it is constructed based on the desired velocity, which is available, and the tracking error, which is also measurable only be measuring the clad height. Using Eq. (18) and the reference velocity definition, $\dot{S}$ can be determined as

$$\dot{S} = \dot{h} - \dot{h}_r \tag{19}$$

Since equivalent control is a means for determining the system motion restricted to the sliding surface $S(t)=0$, if the dynamics were exactly known. So at this stage, it is assumed that $\zeta=0$, i.e., the lumped uncertainty term in Eq. (12) and, thus, $\dot{h}=\hat{f}+\hat{b}u(t)$. By substituting $\dot{h}=\hat{f}+\hat{b}u(t)$ into Eq. (19) and from Eq. (18) the following is obtained:

$$u_{\text{eq}} = \hat{b}^{-1}(\dot{h}_r - \hat{f}) \tag{20}$$

The equivalent control law would maintain $\dot{S}=0$ if the dynamics were exactly known. Since, the dynamics is approximately known, the auxiliary terms $u_p(t)$ and $u_a(t)$ are necessary to drive the system trajectory to the prescribed sliding surface and ensure that it remains on sliding surface for all $t \geq t_0$.

4.2 Step 2: Auxiliary Proportional Control Component $u_p(t)$. In the second step, a control law is designed such that it satisfies a sufficient condition for the existence and reachability of sliding mode for nominal system, i.e., $\dot{h}=\hat{f}+\hat{b}u(t)$. One method to design a control law that derives the system trajectories to the sliding surface from any initial condition is to satisfy the sufficient condition for the existence of the sliding mode. The existence of the sliding mode is guaranteed if the following condition is satisfied [10,11].

$$S\dot{S} < 0 \tag{21}$$

Equation (21) can be interpreted as a negative time derivative of a quadratic positive definite Lyapunov function of the nominal system, i.e., $\dot{h}=\hat{f}+\hat{b}u(t)$, and sliding surface described by Eq. (16).

$$V = \frac{1}{2}S^2 \tag{22}$$

where V is a positive definite Lyapunov function. In order to reach the surface in a finite time and guarantee the stability of the system, derivative of Lyapunov function needs to be a negative definite function [16]. Therefore, $\dot{V}$ can be chosen as follows:

$$\dot{V} = S\dot{S} = -SKS \leq 0 \tag{23}$$

where K is a positive definite constant and is a design parameter. From Eq. (23) one can write the following:

$$S(\dot{S} + KS) = 0 \tag{24}$$

substituting $\dot{S}=\dot{h}-\dot{h}_r$ and then $\dot{h}=\hat{f}+\hat{b}u(t)$ in Eq. (24) yields

$$\hat{f} + \hat{b}u(t) - \dot{h}_r + KS = 0 \tag{25}$$

solving Eq. (25) for $u(t)$ yields

$$u(t) = \underbrace{\hat{b}^{-1}(\dot{h}_r - \hat{f})}_{u_{\text{eq}}(t)} + \underbrace{(-\hat{b}^{-1}KS)}_{u_p(t)} \tag{26}$$

The first term of Eq. (26) is equal to $u_{\text{eq}}(t)$ presented in Eq. (20), and the second term can be regarded as an auxiliary term $u_p(t)$ that guarantees the reachability and existence of the sliding mode for nominal system. The auxiliary term $u_p(t)=-\hat{b}^{-1}KS$ can be interpreted as a proportional action of the sliding function. The proportional term $u_p(t)$ is considered to improve the transient performance while the system is in the learning process. As can be seen, $u_p(t)$ is proportional to the value of sliding function (i.e., S). This is also in agreement with practical consideration, which dictates that the control input should be reduced as the state trajectory converge the sliding surface. But, if the control law is designed based on the bound of uncertainties a high control input is imposed for all $t \geq t_0$. It also compensates for the error that may result from the estimation of the uncertainties, which is derived in the following section.

4.3 Step 3. Compensation of Uncertainties $u_a(t)$. In this step, a control component, which accounts for the lumped uncertainties is designed. Considering the system defined by Eq. (12), i.e., $\dot{h}=\hat{f}+\hat{b}u(t)+\zeta$, an adaptive controller component, $u_a(t)$, may be defined such that an estimate of the lumped uncertainty term ζ is generated, which is denoted by ζ_{est}, hereafter. If ζ were known, then including the term $u_a(t)=-\hat{b}^{-1}\zeta$ in the control law would compensate for the effects of all the uncertainties. On the other hand, if ζ_{est} approaches ζ over time, then including $u_a(t)=-\hat{b}^{-1}\zeta_{\text{est}}$ in the control law could compensate for the effects of the uncertainties over time provided that the estimation mechanism is designed properly. Therefore, $u_a(t)$ is a variable (adaptive) term, which is constructed based on online estimation of the uncertainties and defined as follows:

$$u_a(t) = -\hat{b}^{-1}\zeta_{\text{est}} \tag{27}$$

By combining the components derived in the above steps the proposed control law is obtained as

$$u(t) = \underbrace{\hat{b}^{-1}(\dot{h}_r - \hat{f})}_{u_{\text{eq}}(t)} + \underbrace{(-\hat{b}^{-1}KS)}_{u_p(t)} + \underbrace{(-\hat{b}^{-1}\zeta_{\text{est}})}_{u_a(t)}$$

or

$$u(t) = \hat{b}^{-1}(\dot{h}_r - \hat{f} - KS - \zeta_{\text{est}}) \tag{28}$$

In the following section asymptotic stability of the closed-loop system with the above proposed control law is analyzed and proved using Lyapunov method in the presence of the uncertainties. To calculate ζ_{est}, an appropriate estimation mechanism also called update law is derived systematically through the stability analysis.

5 Stability and Robustness Analysis

STABILITY THEOREM. *Consider a nonlinear uncertain dynamical system represented by Eq.* (12), *i.e.,* $\dot{h}=\hat{f}+\hat{b}u(t)+\zeta$. *If the control law of Eq. (28) is applied, robust stability of the closed-loop system in the presence of model uncertainties and disturbances is guaranteed.*

Proof: To prove the robustness and stability of the system, the following Lyapunov function is considered:

$$V = 0.5(S^2 + \Gamma^{-1}E^2) \tag{29}$$

where Γ is a scalar positive constant, which is a design parameter and E is the estimation error and is defined as follows:

$$E = \zeta_{\text{est}} - \zeta \tag{30}$$

where ζ_{est} is the estimated uncertainties and ζ is the unknown uncertainty. In fact, by minimizing the estimation error, the estimated uncertainties (i.e., ζ_{est}) reaches ζ as time tends to infinity. This is shown in what follows. From Eq. (29) the derivative of Lyapunov function is

$$\dot{V} = S\dot{S} + \Gamma^{-1}E\dot{E} \tag{31}$$

Based on Eq. (19) $\dot{S}=\dot{h}-\dot{h}_r$ and from Eq. (30) $\dot{E}=\dot{\zeta}_{\text{est}}-\dot{\zeta}$. Substituting for $\dot{S}$ and $\dot{E}$ into Eq. (31) yields

$$\dot{V} = S(\dot{h} - \dot{h}_r) + \Gamma^{-1}E(\dot{\zeta}_{\text{est}} - \dot{\zeta}) \tag{32}$$

Using Eq. (12), i.e., $\dot{h}=\hat{f}+\hat{b}u(t)+\zeta$ and replacing for $\dot{h}$ in Eq. (32) results in

$$\dot{V} = S(\hat{f} + \hat{b}u(t) + \zeta) - S\dot{h}_r + \Gamma^{-1}E(\dot{\zeta}_{\text{est}} - \dot{\zeta}) \tag{33}$$

Substituting for the control input, i.e., $u(t)=\hat{b}^{-1}(\dot{h}_r-\hat{f}-KS-\zeta_{\text{est}})$, in Eq. (33), and rearranging leads to

$$\dot{V} = -SKS - SE + E\Gamma^{-1}(\dot{\zeta}_{\text{est}} - \dot{\zeta}) \tag{34}$$

Now if the following update law is chosen:

$$\dot{\zeta}_{est} = \Gamma S \tag{35}$$

The proposed estimator stems from the fact that uncertainties influences the sliding function dynamics (S-dynamics), therefore, the integration of $S(t)$ from t_0 to t can be an indication of the time-varying uncertainty. By substituting Eq. (35) into Eq. (34), the following can be obtained:

$$\dot{V} = -SKS - E\Gamma^{-1}\dot{\zeta} \tag{36}$$

The second term of Eq. (36), i.e., $E\Gamma^{-1}\dot{\zeta}$, shows the combined effects of the estimation error, estimation gain, and the rate of change in the uncertainties with respect to time on $\dot{V}$. Since the complete knowledge of the above term is not available, the best one can consider is the worst-case scenario, when $E\Gamma^{-1}\dot{\zeta}<0$. Thus, Eq. (36) can be written as follows:

$$\dot{V} = -SKS - E\Gamma^{-1}\dot{\zeta} \leq -SKS + |E\Gamma^{-1}\dot{\zeta}| \tag{37}$$

$$\dot{V} \leq -K|S|^2 + \frac{|E\dot{\zeta}|}{\Gamma} \tag{38}$$

$$\dot{V} \leq -K|S|^2 + \frac{|E||\dot{\zeta}|}{\Gamma} \tag{39}$$

From Eq. (39), $\dot{V} < 0$ if

$$K|S|^2 > \frac{|E||\dot{\zeta}|}{\Gamma} \tag{40}$$

or equivalently

$$|S| > \left(\frac{|E||\dot{\zeta}|}{\Gamma K}\right)^{1/2} = \delta \tag{41}$$

where $\delta > 0$ is a positive scalar value. Equation (41) implies that $\dot{V}$ is negative definite for all $|S| > \delta$, which means V is bounded and all trajectories will approach the δ vicinity of the sliding surface $S(t)=0$. Thus, all solutions of the closed-loop system are uniformly ultimately bounded. On the other hand, since the magnitude of δ depends on the choice of K and Γ, the designer of the controller can make it arbitrarily small by increasing the design parameters and, hence, the magnitude of $S(t)$ for which $\dot{V}$ is negative definite can be reduced arbitrarily using the design parameters K and Γ in the presence of time-varying uncertainties. Furthermore, in many practical applications the variation in uncertainty with respect to time (i.e., $\dot{\zeta}$) can be considered zero or negligible ([10] page 43). Therefore, for the slowly time-varying cases one can achieve asymptotic stability and Eq. (36) can be written as

$$\dot{V} = -KS^2 \leq 0 \tag{42}$$

which implies that the trajectories asymptotically will converge to surface $S=0$ from any nonzero initial error, and guarantees the robust stability of the closed-loop system. Furthermore, using Barbalat's lemma [10] it can be shown that the closed-loop system is asymptotically stable and the tracking error will converge to zero as time tends to infinity. At this point, to clarify the above discussions, laser cladding process described by Eqs. (7) and (12), and partially known parameters presented in Table 1, is simulated in the presence of the constant and time-varying uncertainties.

$$\dot{h} = -\frac{h}{\hat{\tau}} + \frac{3}{2}\frac{\hat{k}}{\hat{\tau}}\frac{\hat{m}}{\rho w_0}\left(\frac{d_b}{d_p}\left(1 + \frac{h}{d_b}\tan\alpha\right)\cos\alpha\right)^n u(t) + \zeta \tag{43}$$

Case 1. Time-varying uncertainty and sinusoidal form of the desired clad height.

$$h_d = 0.75 + 0.25\sin(1.5t); \quad \zeta = \pm(0.25 + 0.5^*\sin(\pi t)) \tag{44}$$

In Eq. (44), a constant disturbance plus a sinusoidal time-varying term is considered as the uncertainty to resemble parameters uncertainty and fluctuations that may occur in powder delivery system (i.e., fluctuations of powder flow rate). Figures 4(*a*) and 4(*b*) show the convergence of system trajectories to sliding surface in state space and time domain, respectively, and the effect of sign of the lumped uncertainty. Figure 5 shows the chattering-free control input and convergence of clad height to desired clad height with the proposed control law.

Figure 6 shows that by changing the design parameters designer can arbitrarily reduce the tracking error to the desired value.

Case 2. Constant uncertainty and constant clad height (desired trajectory).

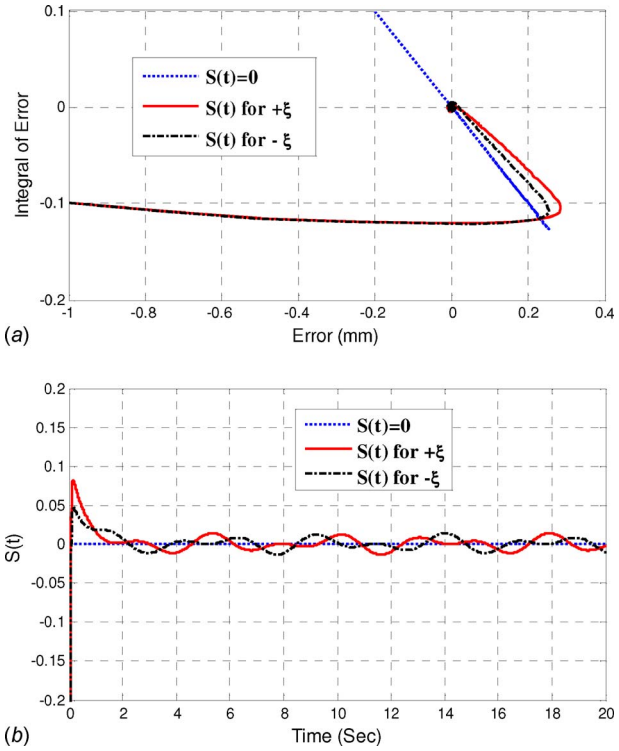

Fig. 4 Convergence of system trajectories to sliding surface: (*a*) system trajectories in state space and (*b*) sliding function behavior in time domain

$$h_d = 1.2; \quad \zeta = \mp 2 \tag{45}$$

In this case a constant uncertainty with positive and negative sign is introduced to show the asymptotic stability and convergence of the system trajectories to an equilibrium point as a result of Eq. (40) for slowly time-varying uncertainties. Figure 7 shows the effect of uncertainty sign. Figures 7 and 8 also show that system trajectories converge to the sliding surface in a finite time and remains on thereafter. Figure 8 illustrates the chattering-free control input and convergence of the clad height to the desired height.

Figures 9 and 10 show the performance of the controller to a step reference height and a disturbance rejection capability of the

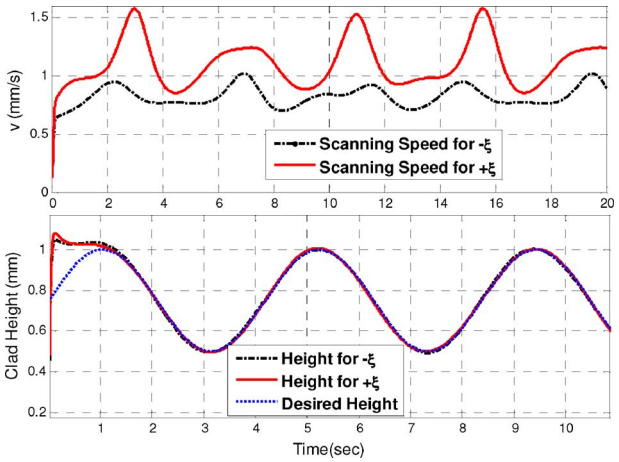

Fig. 5 Chattering-free control input, and convergence of process height to the desired height for time-varying uncertainty

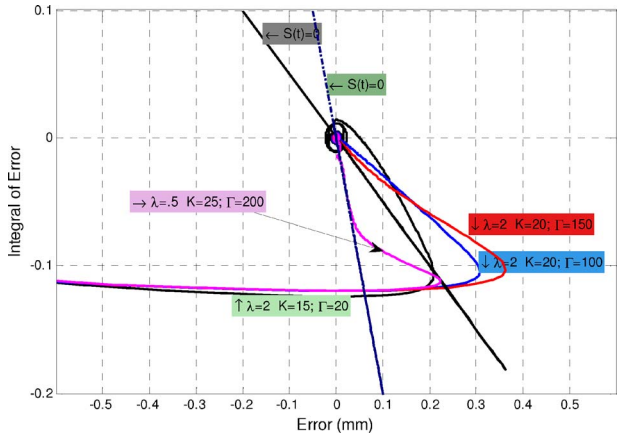

Fig. 6 Comparison of system trajectories convergence

proposed controller when it is disturbed by sudden changes in the height of the clad. From Fig. 10, it can be seen that how $S(t)=0$ converges to $S(t)=0$.

Based on Eq. (35), the lumped uncertainty can be estimated simply by integrating Eq. (35), i.e., $\dot{\zeta}_{est}=\Gamma S$, as follows:

$$\zeta_{est}=\Gamma\int Sdt \tag{46}$$

As mentioned in step 3 of the control design, by replacing estimated uncertainty, i.e., $\zeta_{est}=\Gamma\int Sdt$ in Eqs. (28), i.e., $u(t)=\hat{b}^{-1}(\dot{h}_r-\hat{f}-KS-\zeta_{est})$, the following robust adaptive control law is obtained:

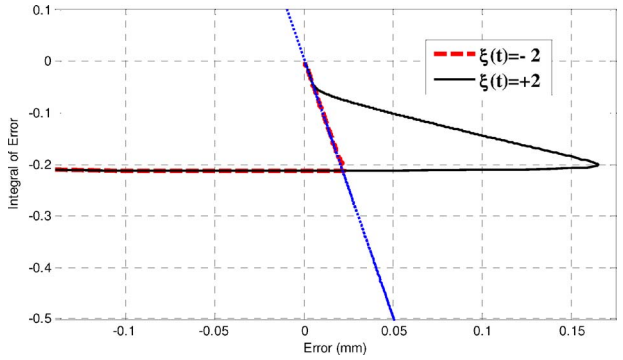

Fig. 7 Convergence of system trajectories to sliding surface

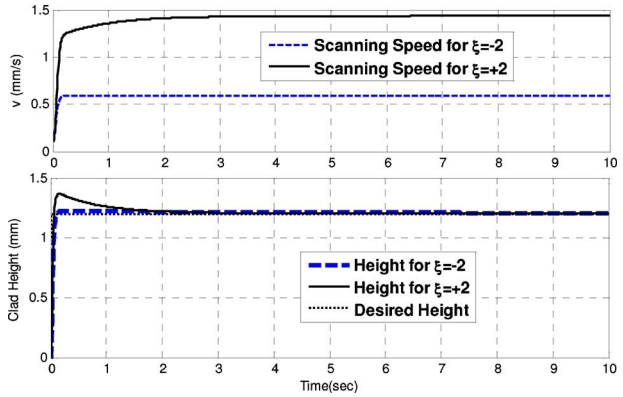

Fig. 8 Chattering-free control input and convergence of clad height to the desired height

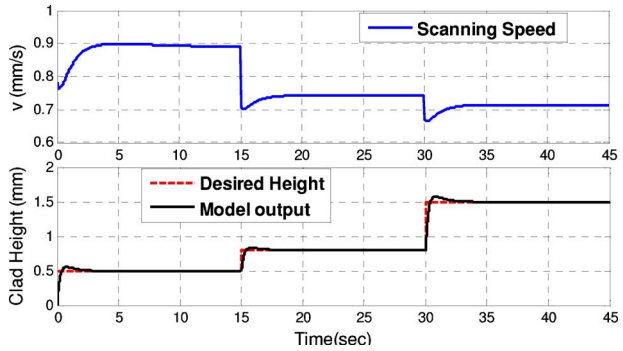

Fig. 9 Controller performance for the step command

$$u(t)=\hat{b}^{-1}\left(\dot{h}_r-\hat{f}-KS-\Gamma\int Sdt\right) \tag{47}$$

The block diagram of the control law presented in Eq. (47) is given in Fig. 11 to illustrate the implementation of the proposed method.

At this point, the analysis of the closed-loop dynamics is discussed to show the effectiveness of the proposed method. The proposed control law of Eq. (47) and the dynamical system given in Eq. (12), i.e., $\dot{h}=\hat{f}+\hat{b}u(t)+\zeta$, lead to the following closed-loop dynamics:

$$\dot{S}+KS=-E \tag{48}$$

$$\dot{S}+KS+\Gamma\int Sdt=\zeta \tag{49}$$

which shows the relation between uncertainties and S-dynamics. By differentiating Eq. (49), one can obtain a second-order differential equation in which time rate of uncertainty act as an input.

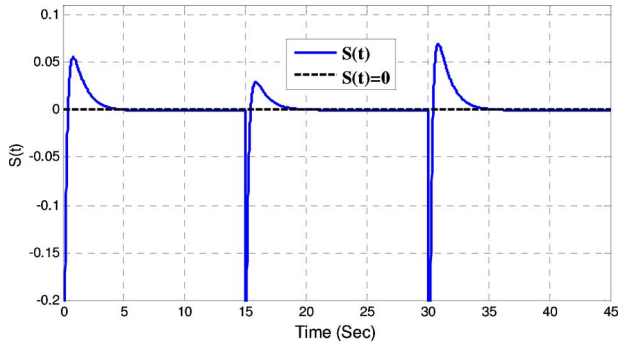

Fig. 10 Convergence of $S(t)$ to zero after a large change in clad height

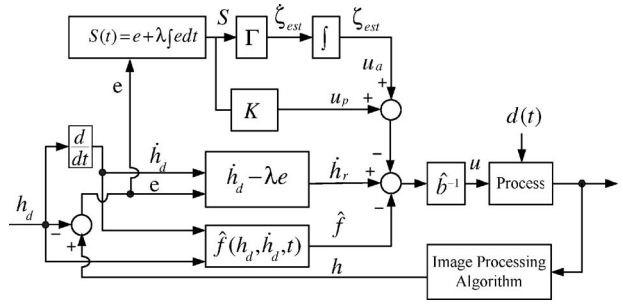

Fig. 11 Block diagram of the proposed controller with uncertainties estimation

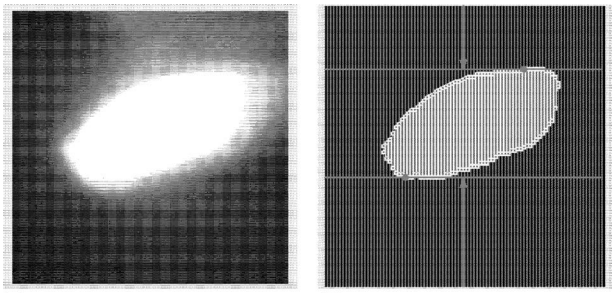

(a) (b)

Fig. 12 Image processing results: (*a*) original image of melt pool and (*b*) processed image of melt pool

Equation (47) provides useful information in order to choose the design parameters K and Γ. As a result, if the sliding mode could be enforced to zero by a properly designed controller then $\dot{S}=0$ as well. Using the definition of $S(t)$ from Eq. (19) yields

$$\dot{e}+\lambda e=0 \tag{50}$$

Equation (50) is just the ideal error dynamics in feedback linearization literature as if the uncertainties did not exist [12]. In fact, Eq. (50) represents an exponentially stable error dynamics. Therefore, if initially $e(0)=\dot{e}(0)=0$ then $e(t)=0$, $\forall t\geq 0$, i.e., a perfect tracking is achieved. Otherwise, $e(t)$ converges to zero exponentially.

Remark 1. The main feature of the proposed ASMC with the derived uncertainties estimation method is that it does not require the knowledge of dynamical system parameters or a priori knowledge of uncertainties' bounds and is based entirely on the desired and actual trajectories, which are both available. Consequently, the complex parameterized dynamic model of the system under consideration with unknown parameters is not required. Therefore, as it is shown in the simulation results presented in Figs. 4–9 with any estimation for $\hat{b}$ (yet bounded and invertible) and $\hat{f}$, the tracking error converges to the desired value.

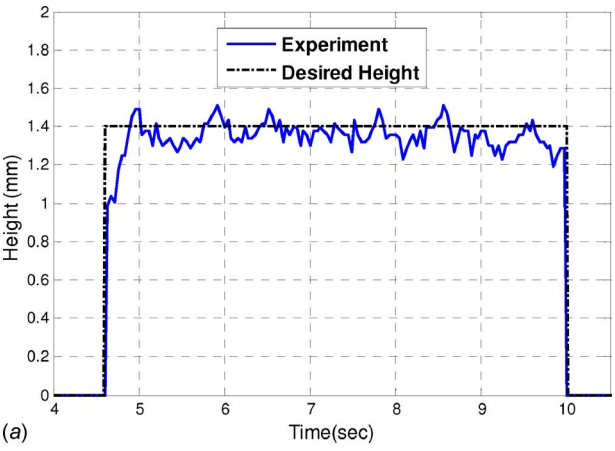

(a)

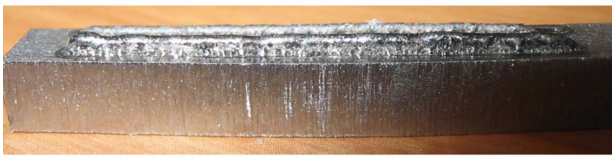

(b)

Fig. 13 Control system performance to a simple linear reference input

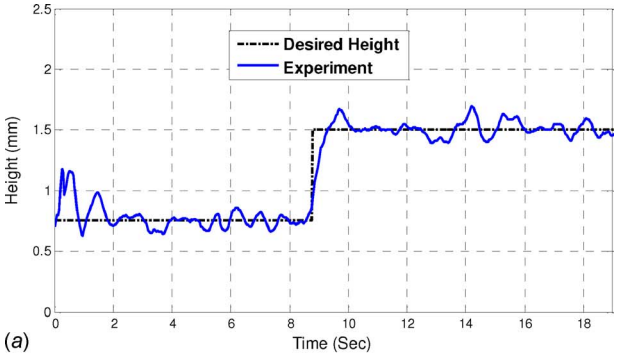

(a)

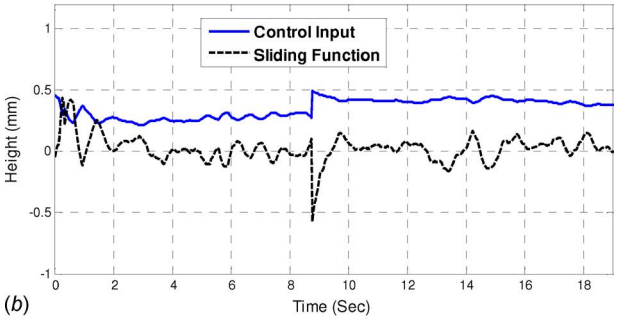

(b)

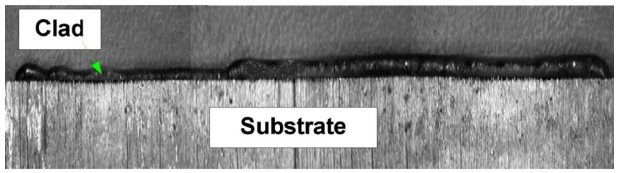

(c)

Fig. 14 Control system performance in tracking step reference input

6 Experimental Results

In this section the experimental results are presented. A series of experiments were designed and carried out to verify and validate the results obtained in previous sections and to show the usefulness of the closed-loop laser cladding. To conduct the experiments, the proposed controller was implemented using LABVIEW graphical platform, MATLAB, and hardware described in Sec. 2. As mentioned earlier, in order to monitor the height of the melt pool, a CCD camera, which is carefully calibrated is used to capture the image of the melt pool. The calibration of the camera is performed using an image of an object with known sizes. At this point, the acquired digital image of the melt pool is fed to an image thresholding toolbox of LABVIEW in order to perform image segmentation and identify the melt pool from the background. Then the melt pool height is obtained using image processing toolbox of MATLAB and LABVIEW. During the experiments, it turned out that monitoring of the melt pool height is very challenging due to the light intensity, and variation in melt pool temperature. To attenuate the high intensity appropriate filters were selected and installed on the camera and image processing algorithm (IMPA). The developed IMPA is able to eliminate the flare and noise to a large extent. As indicated in Fig. 12, after processing of the melt pool image its height is measured. Another aspect that should be considered in the development of the IMPA is the computation burden. It was observed that high computation burden increases the sampling time of the closed-loop system, which in turn can degrade the smoothness of the deposited layers. A sample result of the IMPA is illustrated in Fig. 12.

In the next step of the experiment the proposed control law implemented on the host PC and the output voltage was connected

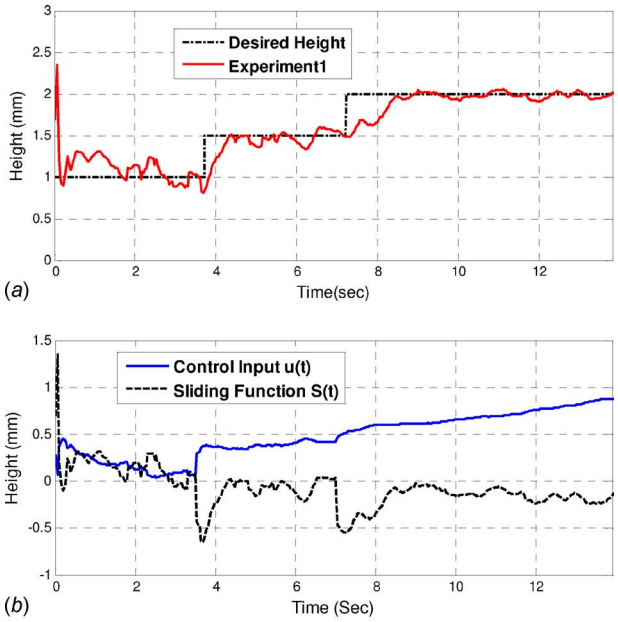

Fig. 15 Control system performance in tracking multiple step reference input

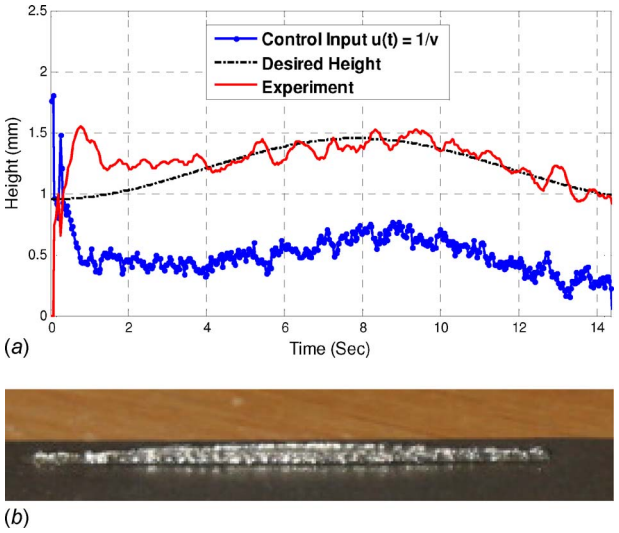

Fig. 16 Control system performance in tracking sinusoidal reference input

to the CNC machine through the analog output of the National Instruments (NI) motion control card to adjust the substrate speed (i.e., scanning speed). Several experiments were designed and carried out using stainless-steel powder. During the experiment different values of laser power were selected and different aspects such as process time, quality of the clad and bounding to substrate were examined. And based on these examinations 350 W was selected for experiment. The powder flow rate is kept at a constant rate of 6 (gr/min) for all the experiments. The powder feed rate of 6 g (r/min) is the lowest value that our powder feeder can deliver with reasonable accuracy. This value is selected to keep the cost of experiments as low as possible.

Case 1. In this experiment, several single layer clads with different reference inputs (desired trajectory) were deposited to show the performance of the IMPA and also the performance of the proposed controller. Figure 13 illustrates the performance of the closed-loop system in tracking a simple linear reference input.

Figures 14(*a*) and 14(*b*) show the tracking performance, chattering-free control input (i.e., $u=1/v(t)$) and convergence of sliding surface to a neighborhood of $S(t)=0$, respectively. The plots of the control input and sliding surface clearly show that chattering is eliminated without using boundary layer method in which the design of boundary layer thickness is a challenging task and needs a priory knowledge of the uncertainties bounds.

Figures 15(*a*) and 15(*b*) illustrate the performance of the closed-loop system in tracking a multiple step reference input and Fig. 16(*a*) indicates the tracking performance of the controller in tracking sinusoidal reference input and chattering-free control input. Figure 16(*b*) shows the real single sinusoidal clad.

In all the above experiments the controller parameters were set to $\lambda=0.75$, $K=0.20$, $\Gamma=8.00$, and were kept constant to evaluate the adaptive capability of the proposed controller. As indicated in the above figures, different trajectories can be tracked with a small tracking error and without requiring tuning the controller, which is an indication of the robustness property of the controller.

Case 2. Since one of the important applications of the laser cladding is surface coating and repair of the damaged parts, in this experiment the capability of the controller to achieve a flat surface despite of having a substrate with damaged surface is investigated. To simulate this situation a substrate with two slots with different depth was selected as shown in Fig. 17.

In this experiment the goal was to deposit a layer of 1.5 mm height. The slots can be considered as external disturbances that control system should maintain the constant height in the presence of these external disturbances. As indicated in Figs. 18(*a*) and 18(*b*) the results are promising. Figure 18(*b*) shows that when the depth of the slot increases there is a small overshoot. The results show that one can obtain a desired flat surface with minimum amount of finishing cut.

7 Conclusion

In this paper, an adaptive sliding mode control method with an uncertainty estimator was developed for the laser cladding process. The stability and robustness of the proposed method were proved in the presence of time-varying uncertainties. The performance of the proposed controller was validated by simulation and experiments. The proposed method uses the advantages of sliding mode and adaptive control techniques while the disadvantages attributed to these methods are remedied by each other. The main contributions of the proposed approach are (i) elimination of the chattering and (ii) estimation of the lumped uncertainty (i.e., ζ) as an uncertain part of the dynamic model. In this study, the lumped uncertainty is estimated based on the measured performance and from the behavior of the sliding mode dynamics instead of using

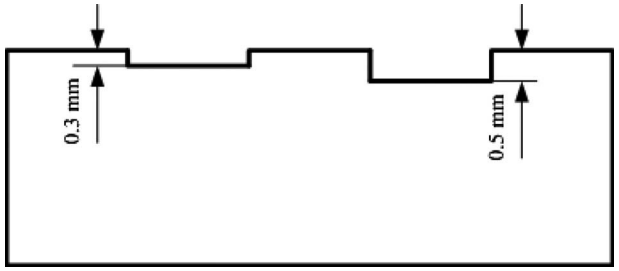

Fig. 17 Substrate with two slots

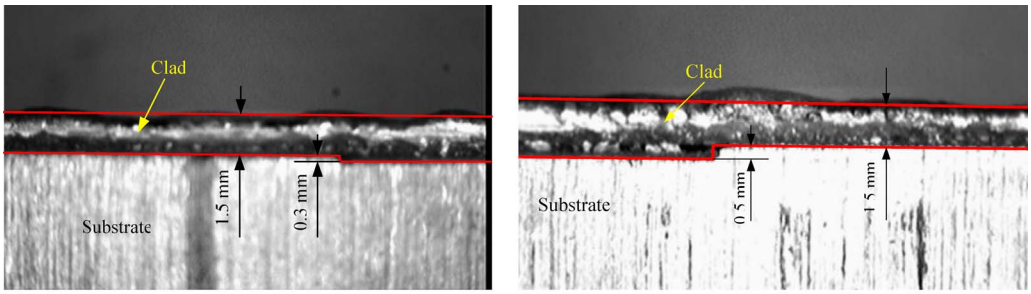

Fig. 18 Deposition of a clad layer on substrate with two slots: (*a*) slot with 0.3 mm and (*b*) slot with 0.6 mm

the conservatively estimated uncertainty bounds to design a robust sliding mode controller. The results obtained in this paper can readily be applied to a control of a multi-input-multi-output nonlinear uncertain dynamical system.

Acknowledgment

The authors would like to acknowledge the financial support of Ontario Ministry of Research and Innovation, Natural Sciences and Engineering Research Council of Canada (NSERC), and Industrial Tooling System.

References

[1] Toyserkani, E., Khajepour, A., and Corbin, S., 2005, *Laser Cladding*, CRS, New York.
[2] Frenk, A., Vandyousefi, M., Wangniere, J.-D., Zryd, A., and Kurz, W., 1997, "Analysis of the Laser-Cladding Process for Stellite on Steel," Metall. Mater. Trans. B, **28**(3), pp. 501–508.
[3] Han, L., and Phatak, K. M., 2004, "Modeling of Laser Cladding With Powder Injection," Metall. Mater. Trans. B, **35**, pp. 1139–1150.
[4] Han, L., and Choi, J., 2003, "Two Dimensional Modeling of Laser Cladding With Droplet Injection," ASME Paper No. HT2003-47295.
[5] Hu, D., and Kovacevic, R., 2003, "Sensing Modelling and Control for Laser Based Additive Manufacturing," Int. J. Mach. Tools Manuf., **43**(1), pp. 51–60.
[6] Chen, H. Y., and Huang, S. J., 2004, "Adaptive Fuzzy Sliding-Mode Control for the Ti6Al4V Laser Alloying Process," Int. J. Adv. Manuf. Technol., **24**, pp. 667–674.
[7] Salehi, D., and Brandt, M., 2006, "Melt Pool Temperature Control Using LabVIEW in Nd:YAG Laser Blown Powder Cladding Process," Int. J. Adv. Manuf. Technol., **29**, pp. 273–278.
[8] Fathi, A., Khajepour, A., Durali, M., and Toyserkani, E., 2008, "Geometry Control of the Deposited Layer in a Non-Planar Laser Cladding Process Using a Variable Structure Controller," ASME J. Manuf. Sci. Eng., **130**(3), p. 031003.
[9] Fathi, A., Khajepour, A., Toyserkani, E., and Durali, M., 2007, "Clad Height Control in Laser Solid Freeform Fabrication Using a Feedforward-PID Controller," Int. J. Adv. Manuf. Technol., **35**(3–4), pp. 280–292.
[10] Slotine, J. J., and Li, E. W., 1991, *Applied Nonlinear Control*, Prentice-Hall, Englewood Cliffs, NJ.
[11] Young, K. D., Utkin, V. I., and Ozguner, U., 1999, "A Control Engineer's Guide To Sliding Mode Control," IEEE Trans. Control Systems Technol., **7**(3), pp. 328–342.
[12] Utkin, V. I., 1977, "Variable Structure Systems With Sliding Modes," IEEE Trans. Autom. Control, **22**(2), pp. 212–222.
[13] Elmali, H., and Olgac, N., 1992, "Theory and Implementation of Sliding Mode Control With Perturbation Estimation," IEEE International Conference on Robotics and Automation, Vol. 3, pp. 2114–2119.
[14] Kim, N., Lee, C. W., and Chang, P. H., 1998, "Sliding Mode Control With Perturbation Estimation: Application to Motion Control of Parallel Manipulators," Control Eng. Pract., **6**(11), pp. 1321–1330.
[15] Zeinali, M., and Notash, L., 2006, "Chattering-Free Sliding Mode Control Design Using Fuzzy Modelling and Implementation on Robot Manipulators," Proceedings of CSME Forum.
[16] Jezernik, K., 1996, "Robust Chattering-Free Sliding Mode Control of Servo Drives," Int. J. Electron., **80**(2), pp. 169–179.
[17] Dinda, G. P., Dasgupta, A. K., and Mazumder, J., 2009, "Laser Aided Direct Metal Deposition of Inconel 625 Superalloy: Microstructural Evolution and Thermal Stability," Mater. Sci. Eng., A, **509**, pp. 98–104.
[18] Weerasinghe, V. M., and Steen, W. M., 1983, *In Transport Phenomena in Materials Processing*, M. Chen, J. Mazumder, and C. Tucker, eds., ASME, New York, NY, pp. 15–23.
[19] Hoadley, A., and Rappaz, M., 1992, "A Thermal Model of Laser Cladding by Powder Injection," Metall. Trans. B, **23**, pp. 631–42.
[20] Gutman, S., 1979, "Uncertain Dynamical Systems: A Lyapunov Min-Max Approach," IEEE Trans. Autom. Control, **24**(3), pp. 437–443.
[21] Zak, H. S., 2003, *Systems and Control*, Oxford University Press, New York.